

Study on Dynamic Prediction of Two-Phase Pipe Flow in Inclined Wellbore with Middle and High Yield

Xiaoya Feng^{1, 2}, Wei Luo^{1, 2, *}, Yu Lei³, Yubin Su⁴ and Zhigang Fang³

Abstract: Gas-liquid two-phase flow is ubiquitous in the process of oil and gas exploitation, gathering and transportation. Flow pattern, liquid holdup and pressure drop are important parameters in the process of gas-liquid two-phase flow, which are closely related to the smooth passage of the two-phase fluid in the pipe section. Although Mukherjee, Barnea and others have studied the conventional viscous gas-liquid two-phase flow for a long time at home and abroad, the overall experimental scope is not comprehensive enough and the early experimental conditions are limited. Therefore, there is still a lack of systematic experimental research and wellbore pressure for gas-liquid two-phase flow under the conditions of middle and high yield and high gas-liquid ratio in conventional viscosity, and the prediction accuracy is low. In view of this, this study carried out targeted systematic research, and from the flow pattern, liquid holdup and pressure drop aspects, established the relevant model, obtained a set of inclined wellbore gas-liquid two-phase pipe flow dynamic prediction method. At the same time, firstly, the model is tested by experimental data, and then the model is compared and verified by a number of field measured wells, which proves that the model is reliable and the prediction accuracy of wellbore pressure is high.

Keywords: Flow pattern, middle and high yield, inclined wellbore, systematicness, pressure drop prediction.

1 Introduction

In the engineering technology of oil and gas recovery in complex carbonate reservoirs, there are some technical problems such as low lifting efficiency in the production process, which are affected by complex factors such as reservoir type, wellbore condition and high production. Wellbore is the channel of oil and gas from stratum to ground, and it is the key part to

¹ School of Petroleum Engineering, Yangtze University, Wuhan, 430100, China.

² The Multiphase Flow Laboratory of Gas Lift Innovation Center, CNPC, Wuhan, 430100, China.

³ Gas Lift Test Base of CNPC, Shanshan, 838202, China.

⁴ Oil and Gas Technology Research Institute, Changqing Oilfield Branch Company of CNPC, Xi'an, 710021, China.

* Corresponding Author: Wei Luo. Email: luoruichang@163.com.

Received: 08 September 2019; Accepted: 17 October 2019.

implement oil and gas field development strategy and control. The dynamic prediction of wellbore fluid flow is the core theoretical technology of oil and gas recovery. In the process of oil and gas exploitation, 60%-80% of energy loss is in the wellbore. It is necessary to reasonably design tubing diameter, optimize production of oil and gas wells, predict blowout shutdown period, optimize artificial lifting mode and working parameters. Accurate prediction of wellbore flow performance is an important basis for these works.

Over the years, although gas-liquid two-phase pipe flow has been extensively studied, most of the studies are focused on horizontal flow or vertical flow. Some good correlative rules have been obtained for the calculation of pressure drop and liquid holdup in horizontal flow and vertical flow. However, when these laws are applied to inclined flows, they are often unsuccessful [Chen and Chen (2010)]. With the increasing number of inclined wells, the study of inclined gas-liquid two-phase pipe flow has also been paid more attention.

In 1973, Beggs et al. [Beggs and Brill (1973)] based on the pressure gradient equation derived from the energy conservation equation of homogeneous flow, carried out numerous experiments in a 15 meters inclined transparent pipe with air-water mixtures, and obtained the correlation rules of liquid holdup and resistance coefficient. This method first calculated the horizontal pipeline flow, and then used the tilt correction coefficient to determine the corresponding tilted pipeline flow. This is one of the classical tilted multiphase pipeline flow methods obtained earlier, and it is still widely used today. In 1985, Mukherjee et al. [Mukherjee and Brill (1985)] made regression analysis on the data of more than 1500 groups of pipelines with upstream and downhill gradients, gave the liquid holdup correlation formula applicable to any angle, and gave the pressure drop calculation formula of each part according to the flow mechanism of different flow patterns. In 1986, Han et al. [Han and Chen (1986, 1989)] in China drew the flow pattern distribution map through experimental research, and gave the calculation formulas of void fraction and pressure drop for different flow patterns. In addition, Brill et al. [Brill and Beggs (1986)], Barnea [Barnea (1986, 1987)], Kaya et al. [Kaya, Sarica and Brill (1999, 2001)], Gomez et al. [Gomez, Shoham, Schmidt et al. (2000)] and so on have also given the correlative formulas of inclined gas-liquid two-phase pipe flow. However, the existing methods for calculating pressure drop and liquid holdup of inclined gas-liquid two-phase flow are mostly empirical and semi-empirical methods, and the experimental research only considers the situation of low production, which has great limitations, as shown in Tab. 1 below. In particular, there are very few experimental studies under the conditions of middle and high yield and high gas-liquid ratio, and verification of measured data from multiple wells also shown the limitations [Zhou, Zhu, Zhang et al. (2016)]. Therefore, the experimental study of gas-liquid two-phase pipe flow with different inclination angles at middle and high yield should be carried out to systematically study it. It is necessary to establish a dynamic prediction method for gas-liquid two-phase pipe flow in inclined wellbore to solve technical problems such as low accuracy of wellbore pressure prediction with high gas-liquid ratio. It has important

Table 1: Experimental conditions for inclined gas-liquid two-phase flow

Computing method	Experimental condition				Model type	
	Volume flow of the liquid phase, m ³ /s	Volume flow of the gas phase, m ³ /s	Pipe diameter, mm	Flow medium	Empirical	Mechanism
Beggs-Brill	0-0.0019	0-0.0980	25.4-38.1	air, water	√	
Mukherjee-Brill	0-0.0019	0-0.0980	38	air, kerosene, lubricating oil	√	
DPI	0-0.0005	0-0.0042	15.48-22.31	air, water	√	
Barnea	0-0.0137	0-0.0253	24	air, water		√
Kaya	0-0.0091	0-0.0182	76.2	air, water		√
Gomez	0-0.0049	0.0138-7.5528	54.635-1778	air, oil, water		√

guiding significance for making reasonable working system and optimizing development plan of oil and gas field.

2 Experimental device and method

2.1 Experimental device

The experiment was carried out on the laboratory platform of multiphase flow in Yangtze University. The experiment is equipped with gas flowmeter, temperature sensor, pressure sensor, plunger metering pump and data acquisition module, which can collect all parameters in the experiment in real time and dynamically. The experimental device realizes visualization, and ensures the correctness of data by combining computer acquisition, high-speed camera, manual recording and naked eye observation. The main process of the experiment is: the liquid in the mixing tank is mixed with the compressed gas from the compressor after pressurization, stabilization, measurement and then into the test section. Finally, the gas is separated by the gas-liquid separator and returned to the mixing tank. The gas from the test section is directly discharged into the atmosphere. The layout of the experimental platform is shown in Fig. 1 below.

2.2 The experimental method

In the experiment, a pipe segment with an inner diameter of 60 mm was selected, and air and water were used as the flowing medium. During the experiment, a fixed liquid flow rate is maintained, which is achieved by setting a fixed liquid volume flow rate through the control system. Then adjusted the different volume flow rates of gas, and observed carefully until the gas-liquid flow tends to be stable. Relevant data such as gas flow rate, liquid flow rate, pressure and temperature of each pipe segment in this process were recorded every 5 s, and total of 180 s. Finally, the average value of each measurement parameter was

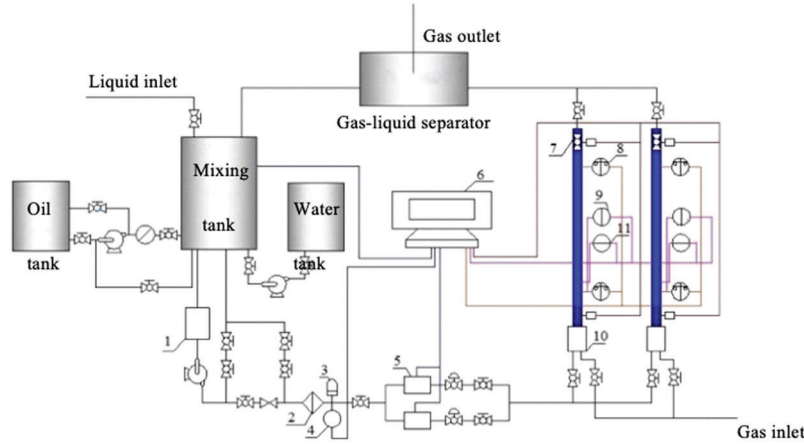


Figure 1: Multiphase flow test device diagram. 1-Liquid flowmeter; 2-Filter; 3-Accumulator; 4-Pressure sensor; 5-Liquid flowmeter; 6-Control acquisition system; 7-Quick closing valve; 8-Differential pressure sensor; 9-Pressure sensor; 10-Gas-liquid mixer; 11-Temperature sensor

taken. After the instrument is closed, the remaining liquid volume in the pipe is measured by using the quick closing valve at both ends of the experimental pipe section, and the liquid holdup is calculated. To avoid contingency, each group of experiments were carried out three times. After one set of experiments, the liquid flow rate and inclination angle were changed to carry out the next set of experiments.

The purpose of the design experiment is to obtain the liquid holdup and pressure drop under the corresponding conditions when the gas-liquid ratio and inclination angle are changed, so as to provide data support for the next calculation. The data range of the experiment is shown in Tab. 2 below. Compared with the data range of Tab. 1, the liquid volume flow and gas volume flow of the experiment are higher, and the gas-liquid ratio is also larger.

3 Experimental analysis

3.1 Flow pattern

3.1.1 Flow pattern contrast

In the study of multiphase flow, in order to characterize the influence of pipe diameter, flow rate, gas-liquid ratio, pressure, temperature and other parameters on the flow pattern and

Table 2: Range of experimental data

Pipe diameter, mm	Flow medium	Volume flow of the liquid phase, m ³ /d	Volume flow of the gas phase, m ³ /d	Inclination angle, °
60	air, water	50, 100, 150, 200, 250, 300, 350, 400, 450, 500	5000, 10000, 15000, 20000, 25000, 30000, 35000, 40000, 45000, 50000	15, 30, 45, 60, 75, 90

pressure drop, the superficial velocities of liquid and gas are generally used to analyze and study the flow law of multiphase flow [Han, Zhang, Xu et al. (2015); Zhang (2015)].

In 1999, Kaya et al. [Kaya, Sarica and Brill (1999)] studied gas-liquid two-phase flow in inclined wells on the basis of previous studies, and presented a comprehensive mechanical model. The model includes five flow patterns: bubble flow, dispersed bubble flow, slug flow, agitation flow and annular flow. Kaya et al. 's flow pattern prediction model combined their own bubble-flow transition model, Barnea et al. 's dispersed bubble-flow transition model, Tengesdal et al. [Tengesdal, Kaya and Sarica (1999)] 's agitation flow transition model and Ansari et al. 's annular flow transition model.

In order to get the law of flow state change under different inclination angles and gas-liquid ratios, take the liquid superficial velocity as the vertical coordinate, the gas superficial velocity as the horizontal coordinate, and adopt the logarithmic coordinate. According to fluid physical property, pressure, temperature, pipe diameter and other conditions of the experiment, data points of experimental with Kaya flow pattern diagram were obtained by calculating transition boundary between different flow patterns, as shown in Fig. 2 below. In the experiment, there are three flow patterns of inclined pipe, which are slug flow, agitation flow and annular flow. It can be seen from Fig. 2 that the Kaya flow pattern diagram is judging the annular flow as the agitation flow, which is not suitable for the identification of inclined wellbore flow pattern with middle and high yield and high gas-liquid ratio. Therefore, the transition boundary of the flow patterns needs to be reclassified.

3.1.2 Repartition of flow patterns

On the basis of drawing lessons from the flow pattern demarcation limits given by various scholars, the demarcation boundaries between different flow patterns under experimental conditions are given.

(1) Transition between slug flow and agitation flow

Tengesdal et al. [Tengesdal, Kaya and Sarica (1999)] studied the agitation flow in detail and established a new transition criterion suitable for straight and inclined wellbores according to the drift flow method. The total void fraction of slug unit was defined as:

$$\phi_{su} = \frac{v_{sg}}{1.2v + v_0} \quad (1)$$

where, v_{sg} is gas superficial velocity, m/s; v is average velocity of mixture, m/s; v_0 is the rising velocity of Taylor bubble, m/s.

In the equation, the rising velocity of Taylor bubble v_0 is given by Bendiksen [Bendiksen (1984)], namely:

$$v_0 = (0.35 \sin \theta + 0.54 \cos \theta) \left[\frac{g(\rho_l - \rho_g)D}{\rho_l} \right]^{0.5} \quad (2)$$

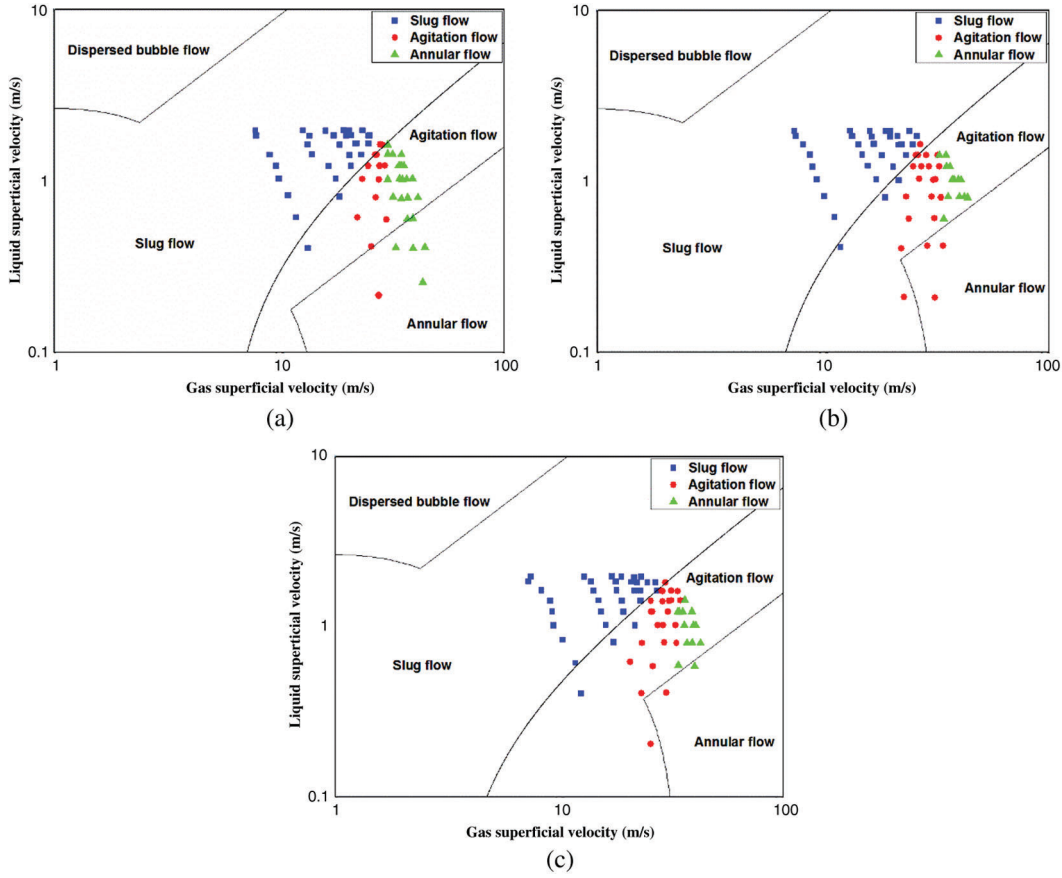


Figure 2: Kaya flow pattern diagram of flow pattern experimental data with different inclination angles. (a) 30°, (b) 60° and (c) 90°

where, ρ_l is the density of liquid phase, kg/m^3 ; ρ_g is the density of gas phase, kg/m^3 ; θ is the angle between the test section and the horizontal, °; g is gravity acceleration, m/s^2 ; D is diameter of test pipe, m.

Tengesdal et al. proposed that the total void fraction of Taylor bubble region should be replaced by the total void fraction of slug unit to represent the transformation. By substituting ϕ_{su} , the transition boundary from slug flow to agitation flow can be obtained:

$$v_{sg} = \frac{\phi_{su}}{1 - 1.2\phi_{su}} \left(1.2v_{sl} + (0.35 \sin \theta + 0.54 \cos \theta) \left[\frac{g(\rho_l - \rho_g)D}{\rho_l} \right]^{0.5} \right) \quad (3)$$

where, v_{sl} is liquid superficial velocity, m/s.

Kaya adopted Owen’s experimental results, that is, when the total void fraction of Taylor bubble region is about 0.78, the slug flow will transform to the agitation flow, and the boundary between slug flow and agitation flow is obtained as follows:

$$v_{sg} = 12.19 \left(1.2v_{sl} + (0.35 \sin \theta + 0.54 \cos \theta) \left[\frac{g(\rho_l - \rho_g)D}{\rho_l} \right]^{0.5} \right) \quad (4)$$

The slug flow and agitation flow observed in the experiment were drawn on the same graph with the transition boundary of slug flow and agitation flow, as shown in Fig. 3 below.

It can be seen from Fig. 3 that the transition boundary of slug flow and agitation flow is basically consistent with the observed slug flow and agitation flow transition under experimental conditions.

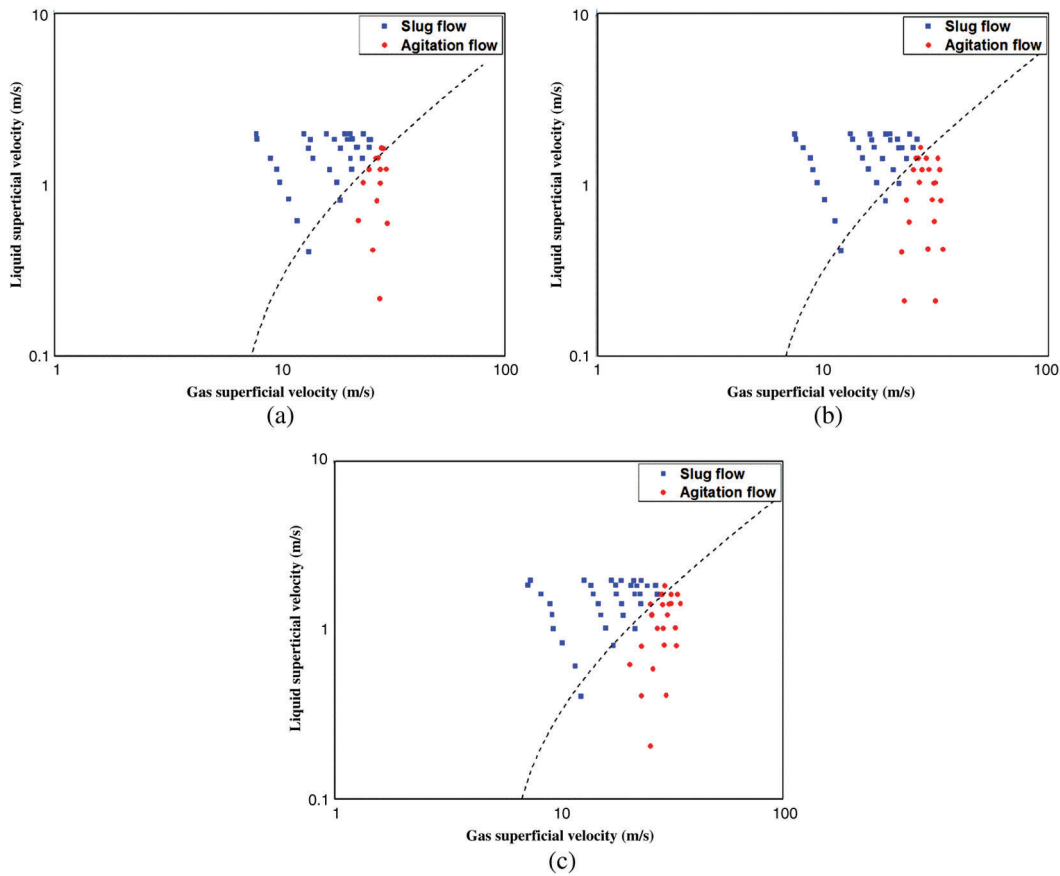


Figure 3: The transition boundary of slug flow and agitation flow with different inclination angles. (a) 30°, (b) 60° and (c) 90°

(2) Transition between agitation flow and annular flow

Hasan et al. [Hasan and Kabir (1988); Kabir and Hasan (1990)] obtained discriminant criterion and proposed a method for distinguishing agitation flow and annular flow by analyzing the mechanism of flow pattern transition of gas-liquid two-phase flow in the vertical pipe. When the gas velocity is high enough, one part of the liquid moves up the pipe wall and the other part exists in the gas core as droplets. When the gas velocity is higher than a certain value, the droplets will be carried out of the wellbore. This critical value can be used to distinguish the transition boundary between the agitation flow and the annular flow. According to the balance principle of droplet between drag force and gravity, combined with the research results of Turner and Taitel, it can be concluded that in the vertical wellbore, the transition boundary of flow pattern is as follows:

$$v_{sg} > 3.1 \left[\frac{\sigma g (\rho_l - \rho_g)}{\rho_g^2} \right]^{0.25} \quad (5)$$

This boundary is only applicable to vertical pipes. Angle should be considered in the experiment. Therefore, the average value of flow pattern transformation under different angles are used to fit the formula, and then the transition boundary between agitation flow and annular flow is obtained. The gas superficial velocity transformed by agitation flow and annular flow with different inclination angles are shown in Tab. 3 below.

Table 3: The gas superficial velocity transformed by agitation flow and annular flow with different angles

Inclination angle, °	15	30	45	60	75	90
V _{sg} , m/s	29.98	29.76	24.41	24.76	24.35	24.67

After fitting, the transition boundary between agitation flow and annular flow is:

$$v_{sg} = 9.72 \left[\frac{\sigma g (\rho_l - \rho_g) \sin \theta}{\rho_g^2} \right]^{0.25} \quad (6)$$

The agitation flow and annular flow observed in the experiment were drawn on the same graph with the fitted transition boundary of agitation flow and annular flow, as shown in Fig. 4 below.

3.2 Analysis of influencing factors of liquid holdup and pressure drop

3.2.1 Analysis of influencing factors of liquid holdup

The variation rule of liquid holdup is shown in Fig. 5 below. At the same liquid volume flow rate, liquid holdup decreases with the increase of gas volume flow rate [Zhang, Wang, Sarica et al. (2003)]. When the gas volume flow rate is greater than 620 m³/h, the liquid holdup

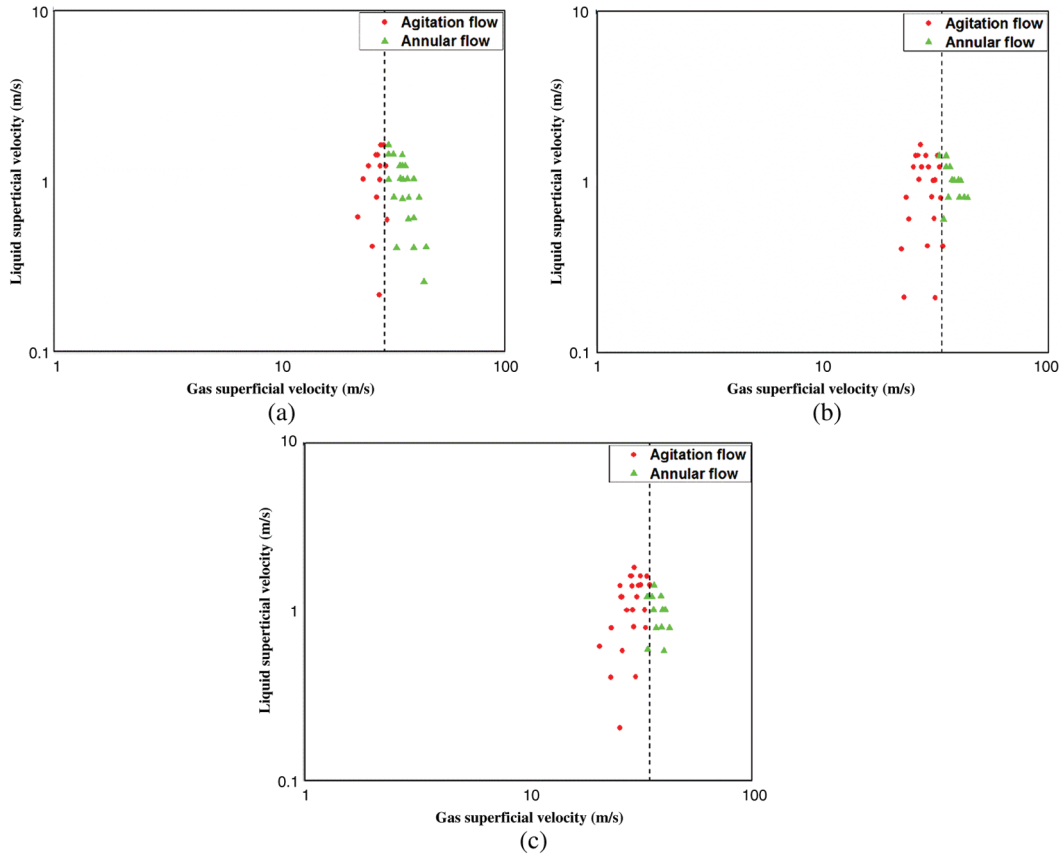


Figure 4: The transition boundary of agitation flow and annular flow with different inclination angles. (a) 30°, (b) 60° and (c) 90°

decreases slowly. The reason is that when the gas volume flow rate is large, the flow pattern changes to the annular flow, and the liquid holdup rate is very low. Increasing the gas volume flow rate has a little impaction on the liquid holdup. At the same gas volume flow rate, the liquid holdup increases with the increase of liquid volume flow rate. Under the same volume flow rate of gas and liquid, with the increase of inclination angles, the liquid holdup presents a trend of first rising and then falling, reaching the maximum value at the inclination angle of about 45°, and then decreases slightly with the increase of inclination angles.

(a) when the liquid volume flow rate is 8.29 m³/h, the liquid holdup changes at different inclined angles; (b) when the liquid volume flow rate is 16.67 m³/h, the liquid holdup changes at different inclined angles; (c) when the gas volume flow rate is 210 m³/h, the liquid holdup changes at different liquid volume flow rates; (d) when the gas volume flow rate is 620 m³/h, the liquid holdup changes at different liquid volume flow rates; (e)

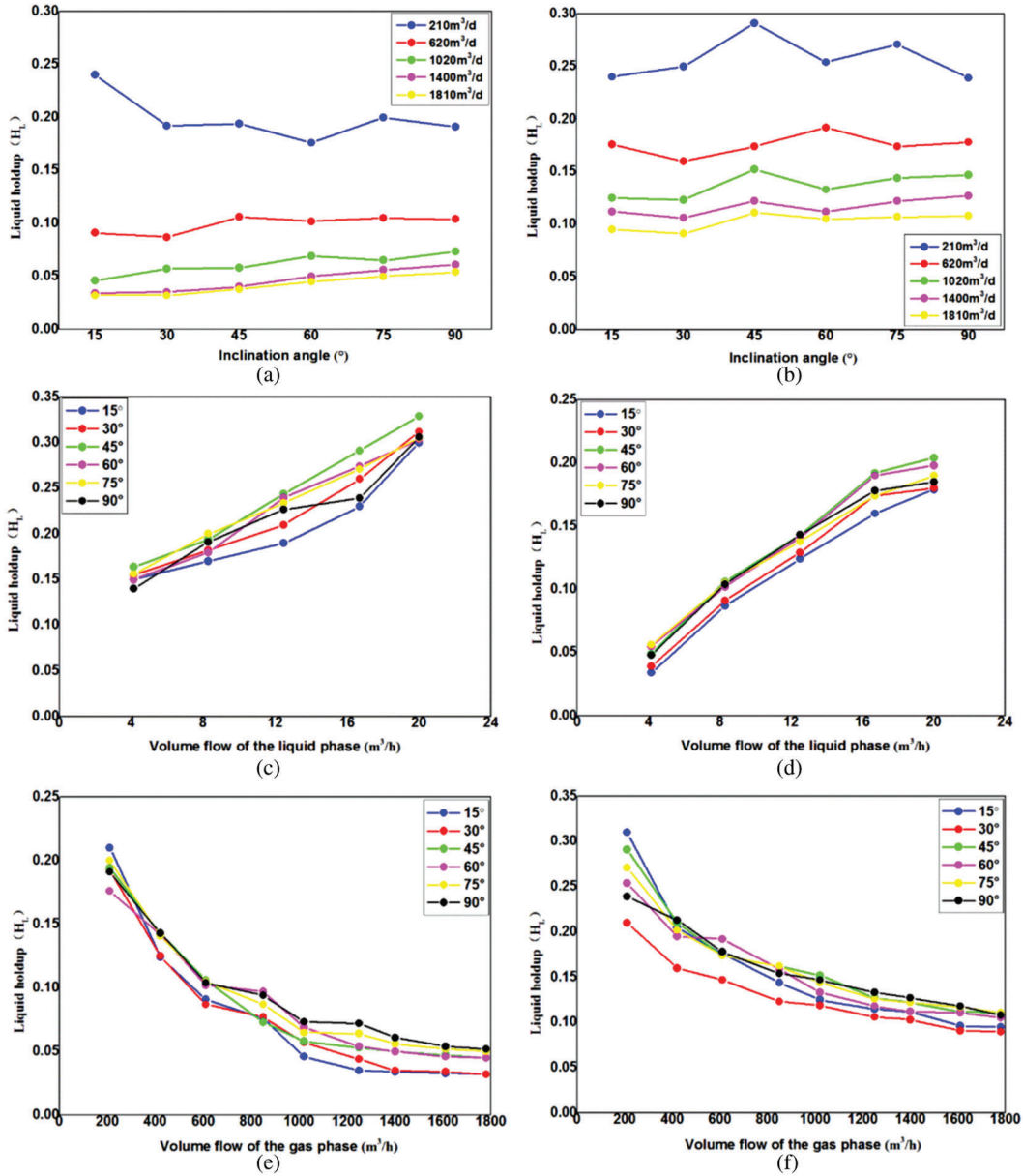


Figure 5: Variation rule of liquid holdup

when the liquid volume flow rate is 8.29 m^3/h , the liquid holdup changes at different gas volume flow rates; (f) when the liquid volume flow rate is 16.67 m^3/h , the liquid holdup changes at different gas volume flow rates.

3.2.2 Analysis of influencing factors of pressure drop

The variation rule of pressure drop is shown in Fig. 6 below. At the same gas volume flow rate, the pressure drop increases with the increase of liquid volume flow rate. At the same liquid volume flow rate, the pressure drop increases with the increase of gas volume flow rate. When the inclination angle is greater than 60°, the pressure drop increases slowly. The reason is that when the inclination angle is between 0° and 60°, the pressure drop of gravity term gradually increases, and the total pressure drop increases with the increase of the inclination angles. When the inclination angle is greater than 60°, although the pressure drop of gravity term gradually increases, the liquid carrying capacity of gas increases, liquid holdup decreases (in Fig. 5), and the total pressure drop decreases.

(a) when the gas volume flow rate is 210 m³/h, the pressure drop changes at different inclined angles; (b) when the gas volume flow rate is 620 m³/h, the pressure drop changes at different inclined angles; (c) when the liquid volume flow rate is 8.29 m³/h,

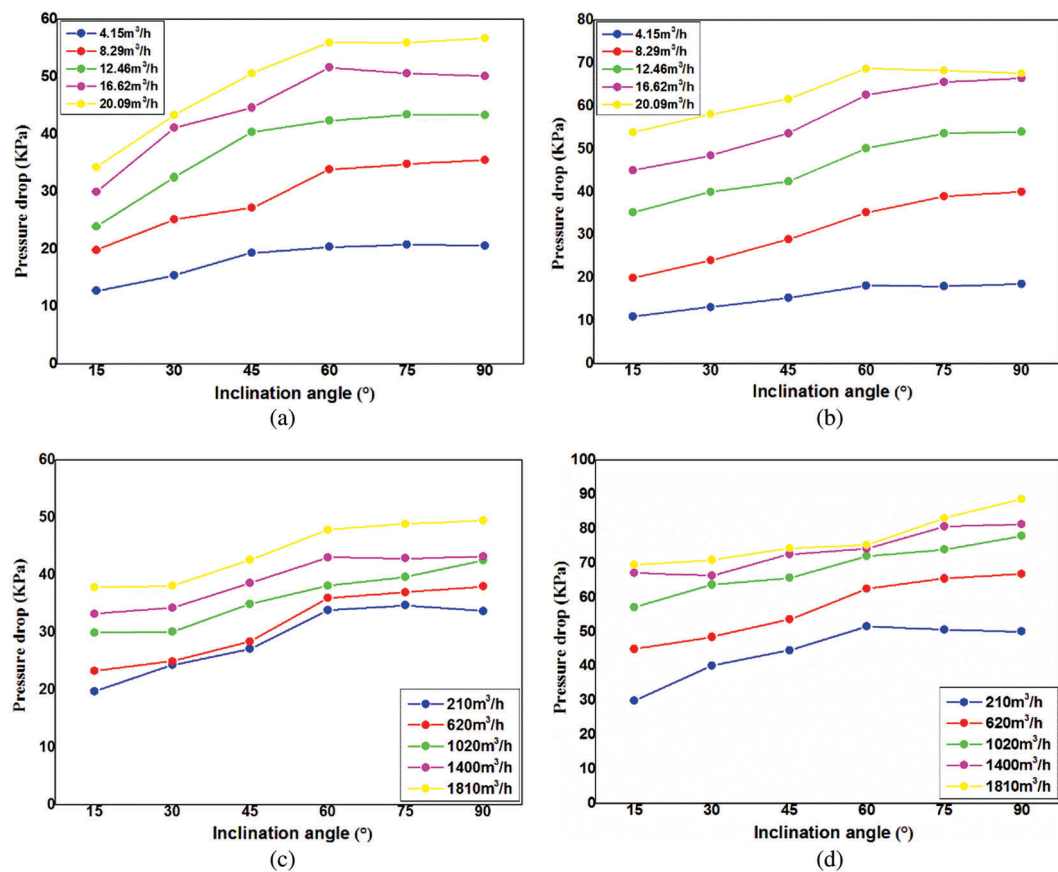


Figure 6: Variation rule of pressure drop

the pressure drop changes at different inclined angles; (d) when the liquid volume flow rate is 16.67 m³/h, the pressure drop changes at different inclined angles.

3.3 A new model for calculating liquid holdup and pressure drop

The total pressure gradient $\frac{dp}{dz}$ of inclined gas-liquid two-phase pipe flow is composed of friction pressure gradient $\left(\frac{dp}{dz}\right)_{fr}$, heavy pressure gradient $\left(\frac{dp}{dz}\right)_h$ and accelerating pressure gradient $\left(\frac{dp}{dz}\right)_a$. According to Beggs-Brill's derivation (Mukherjee uses the same calculation method) [Liang (2019)], we can obtain the following formula for the total pressure gradient:

$$-\frac{dp}{dz} = \frac{[\rho_l H_l + \rho_g(1 - H_l)]g \sin \theta + \frac{\lambda G v}{2DA}}{1 - \{[\rho_l H_l + \rho_g(1 - H_l)]v v_{sg}\}/p} \quad (7)$$

where, p is the absolute average pressure of pipeline, Pa; z is the distance of axial flow, m; H_l is liquid holdup, m³/m³; λ is the resistance coefficient, dimensionless; G is the mass flow rate of mixture, kg/s; A is the section area of the test pipe, m².

It can be seen from this formula that in order to calculate the pressure gradient of inclined gas-liquid two-phase flow, it is necessary to study the correlation between liquid holdup H_l and resistance coefficient of two-phase flow.

3.3.1 Calculation of liquid holdup

According to the experimental data, Mukherjee and Brill obtained the correlation law of liquid holdup of gas-liquid two-phase inclined pipe flow through regression analysis,

$$H_l = \exp \left[(c_1 + c_2 \sin \theta + c_3 \sin^2 \theta + c_4 N_l^2) \frac{N_{vg}^{c_5}}{N_{vl}^{c_6}} \right] \quad (8)$$

Among them,

$$N_{vl} = v_{sl} \left(\frac{\rho_l}{g\sigma} \right)^{0.25} \quad (9)$$

$$N_{vg} = v_{sg} \left(\frac{\rho_l}{g\sigma} \right)^{0.25} \quad (10)$$

$$N_l = \mu_l \left(\frac{g}{\rho_l \sigma^3} \right)^{0.25} \quad (11)$$

where, σ is the surface tension of liquid phase, N/m; μ_l is the viscosity of liquid phase, mPa·s; c_1 - c_6 are empirical coefficients.

Table 4: Empirical coefficients

c_1	c_2	c_3	c_4	c_5	c_6
-0.3459	0.1662	-0.0886	2.9531	0.5075	0.2523

The new empirical coefficients obtained by combining experimental data are shown in Tab. 4 below.

3.3.2 Calculation of resistance coefficient

According to the calculation method of Mukherjee and Brill for the resistance coefficient of gas-liquid two-phase along the inclined pipe, the friction coefficient f_m of gas-liquid two-phase mixture is a function of the non-slip friction coefficient f_{ns} :

$$f_m = f_r f_{ns} \quad (12)$$

In this paper, the relationship between the friction coefficient ratio f_r and the experimental data is as follows:

$$f_r = (2.6254 \sin \theta + 0.1165 \cos \theta + 0.1285) H_r \quad (13)$$

Among them, the relative liquid holdup H_r is calculated as follows:

$$H_r = \frac{H'_l}{H_l} \quad (14)$$

$$H'_l = \frac{v_{sl}}{v_{sl} + v_{sg}} \quad (15)$$

The non-slippage friction coefficient f_{ns} is directly calculated according to the method proposed by Mukherjee and Brill:

$$Re_{ns} \leq 2300, f_{ns} = \frac{64}{Re_{ns}} \quad (16)$$

$$Re_{ns} > 2300, f_{ns} = \left[1.14 - 2 \lg \left(\frac{k}{D} + \frac{21.25}{Re_{ns}^{0.9}} \right) \right]^{-2} \quad (17)$$

where, the non-slippage Reynolds number Re_{ns} :

$$Re_{ns} = \frac{v_m \rho_{ns} D}{\mu_{ns}} \quad (18)$$

The non-slippage mixture density ρ_{ns} :

$$\rho_{ns} = (1 - H'_l) \rho_g + H'_l \rho_l \quad (19)$$

The non-slippage mixture viscosity μ_{ns} :

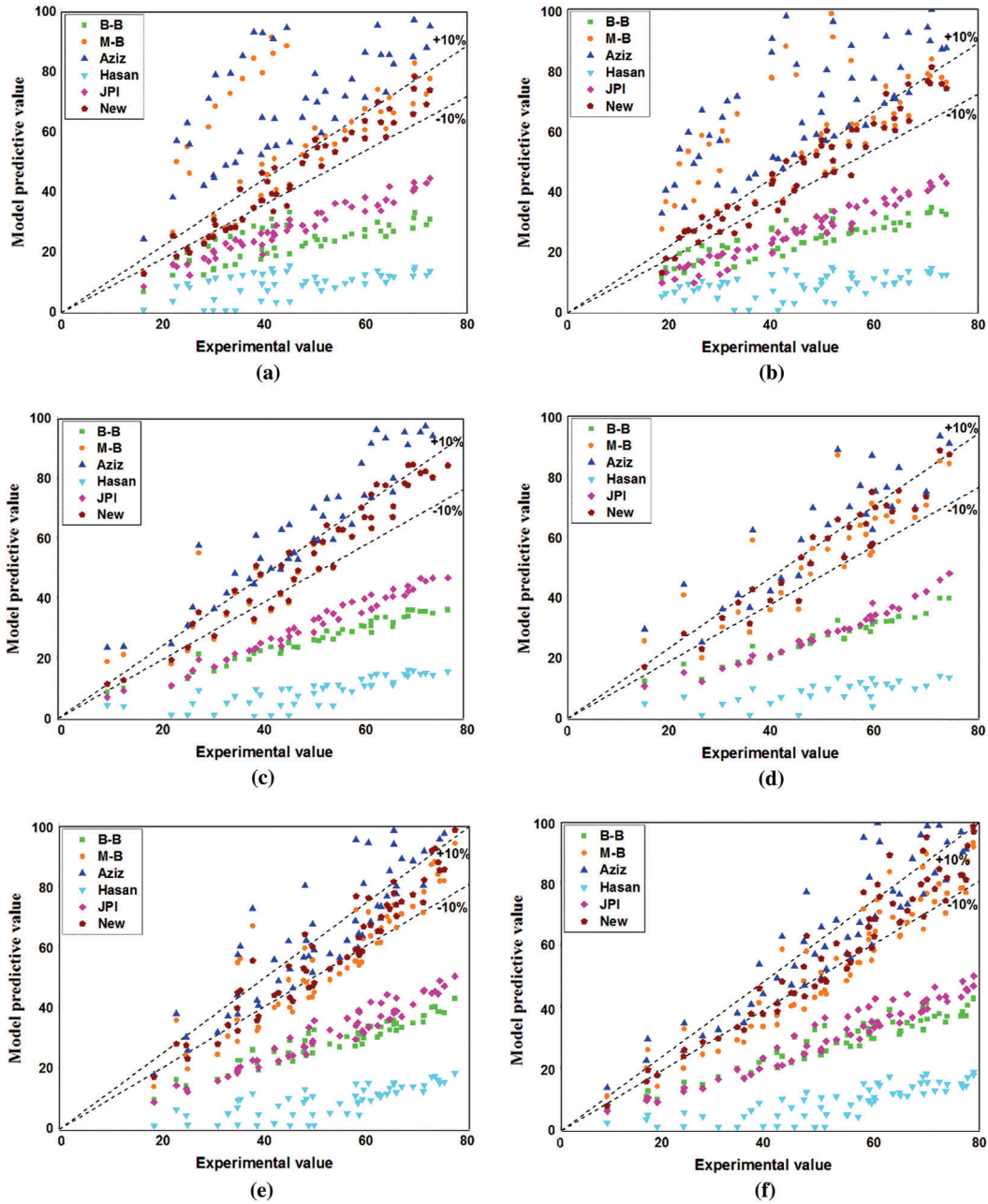


Figure 7: Comparison between the predicted and experimental pressure drop values of different models. (a) 15°, (b) 30°, (c) 45°, (d) 60°, (e) 75° and (f) 90°

Table 5: Prediction errors of different models

Model	Beggs-Brill	Mukherjee-Brill	Aziz	Hasan	JPI	New
Error (%)	48.24	22.72	34.05	82.17	43.58	9.64

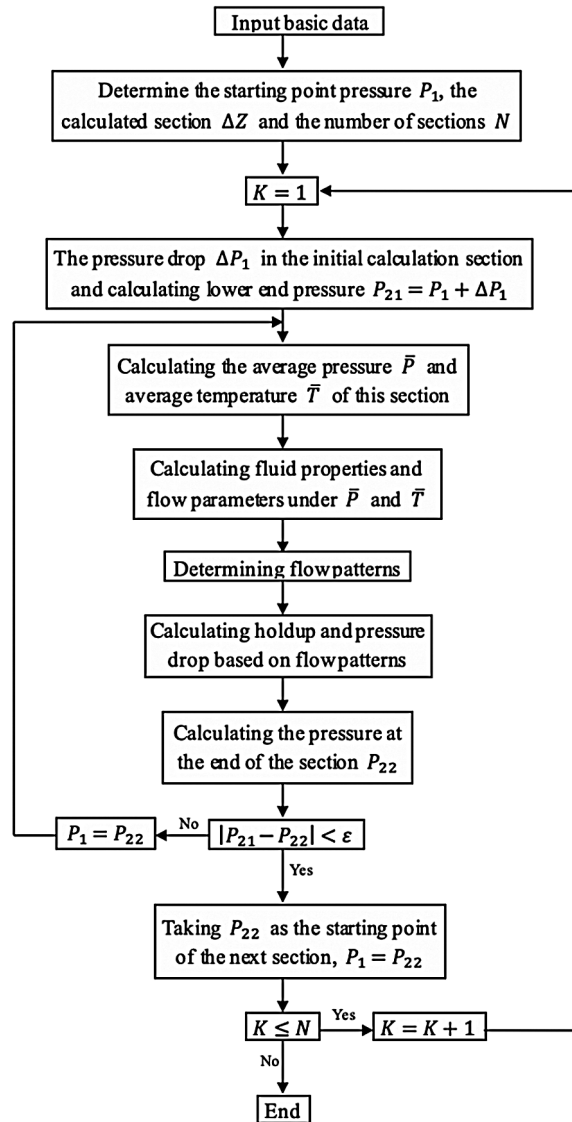


Figure 8: Solution program block diagram

$$\mu_{ns} = (1 - H_l')\mu_g + H_l'\mu_l \quad (20)$$

3.3.3 Evaluation of pressure drop calculation model

The pressure drop data of 15°, 30°, 45°, 60°, 75° and 90° were obtained in the experiment. The comparison between the predicted and experimental pressure drop values of different models are shown in Fig. 7. The models used to predict pressure drop include Beggs-brill (B-B), Mukherjee-Brill (M-B), Aziz, Hasan, JPI, and the new in this paper.

The error results of pressure drop prediction by the above six different models are shown in Tab. 5 below. The prediction error of the new model is about 10%, which indicates that it is better than the other five commonly used models.

4 Verification

4.1 Solution program block diagram

For the above-mentioned mathematical model, the solution program is compiled and calculated. The block diagram of the calculation program is as shown in Fig. 8. To extend the calculation of real wells, the key is to determine the flow pattern, and calculate the liquid holdup and pressure drop by using the correlation on the basis of the flow pattern.

4.2 Verification of field measured data

The biggest obstacle to evaluating the relative laws of inclined gas-liquid two-phase pipe flow with middle and high yield is the lack of field measured data. The production data of 34 measured wells in a certain oilfield are collected, as shown in Tabs. 6 and 7.

Table 6: Range of crude oil physical parameters

Water content (%)	Saturation pressure (MPa)	Crude oil density (g/cm ³)	Formation water density (g/cm ³)	Relative density of natural gas
0-30	7.51, 17.31	0.904, 0.922	1.138-1.144	1.659-1.709, 0.7858

Table 7: Range of production test data

Wellhead pressure (MPa)	Flowing pressure (MPa)	Liquid production (m ³ /d)	Oil production (m ³ /d)	Produced GOR (m ³ /m ³)
1.45-9.31	14.68-26.84	41.65-688.87	41.65-688.87	57.02-677.45

The commonly used pressure drop calculation models and the established new model are compared and verified by a number of field measured wells, and the results are shown in [Tab. 8](#) below. It can be seen that the maximum error, minimum error and average error of the new model calculation are small, which proves that the new model established is reliable and the prediction accuracy of wellbore pressure is high.

Table 8: The results of pressure drop calculation by common models and new model are compared

No.	Orkiszewski	Beggs-Brill	Hasan	Aziz	JPI	Dun-Ros	Hagedorn-Brown	Kaya	New
1	14.44	36.69	17.77	17.7	18.03	34.49	13.91	17.91	12.77
2	12.06	29.7	10.6	10.35	10.91	25.37	11.29	10.92	12.06
3	41.14	10.26	21.35	22.85	27.02	9.37	29.42	25.82	14.68
4	26.26	4.82	18.07	20.83	17.95	12.51	16.84	14.32	16.85
5	11.36	21.09	13.1	12.98	13.37	28.8	10.71	13.39	24.29
6	40.17	8.07	20.3	21.92	25.99	8.62	27.75	24.5	11.2
7	27.25	8.09	18.16	19.64	18.03	12.18	15.53	13.45	15.63
8	26.13	8.85	15.1	16.05	16.97	7.45	18.16	13.85	19.23
9	40.83	11.7	20.57	19.24	25.74	9.16	30.93	26.31	16.88
10	16.52	7.9	9.04	8.04	8.89	11.36	15.87	10.8	6.93
11	21.34	16.82	11.2	7.84	12.61	9.56	6.94	8.51	7.5
12	34.65	7.32	14.96	12.79	18.47	7.78	26.91	21.53	11.09
13	33.06	5.39	7.69	8.57	8.7	20.7	26.5	11.33	5.44
14	13.69	37.88	8.1	8.36	8.27	13.62	5.64	8.03	4.03
15	31.36	19.45	16.55	20.09	19.07	8.05	16.89	11.87	15.95
16	39.16	9.47	16.2	13.87	20.73	7.84	29.82	23.68	13.75
17	28.12	5.35	12.92	13.11	15.95	9.33	21.13	15.96	6.69
18	26.52	6.3	15.82	15.09	17.53	8.61	20.93	16.53	13.21
19	37.26	2.23	13.74	11.61	17.8	8.75	22.62	20.89	2.31
20	24.45	5.89	8.39	7.49	9.35	7.51	20	14.03	6.8
21	10.99	13.9	11.21	11.31	13.48	13.89	10.43	10.62	10.57
22	31.16	10.68	16.26	17.36	19.63	10.58	21.72	17.11	10.12
23	32.34	5.43	8.69	6.79	11.67	12.11	18.91	16.69	6.13
24	29.05	7.93	6.47	6.25	8.13	15.94	16.78	14.38	9.39
25	8.84	8.31	10.31	12.25	11.63	32.7	13.99	5.93	7.09

(Continued)

Table 8 (continued).

No.	Orkiszewski	Beggs-Brill	Hasan Aziz	JPI	Dun-Ros	Hagedorn-Brown	Kaya	New
26	38.9	2.17	11.41	9.33	15.71	9.27	23.82	20.85 1.34
27	28.07	9.68	15.5	14.56	14.64	10.28	25.51	19.66 10.34
28	25.35	8.51	11	10.4	10.71	10.84	22.31	17.25 10.11
29	15.42	16.89	11.79	13.46	11.34	28.37	7.75	5.91 12.5
30	15.42	16.89	11.79	13.46	11.34	28.37	7.75	5.91 12.5
31	34.22	45.23	33.59	34.84	33.56	54.86	15.5	18.12 26.27
32	15.03	21	11.06	12.46	12.07	31.79	5.56	5.28 22.05
33	10.54	33.82	8	8.86	7.26	26.1	35.31	11.06 6.73
34	30.89	9.49	8.74	9.14	10.94	9.95	16.4	10.21 6.44
Maximum	41.14	45.23	33.59	34.84	33.56	54.86	35.31	26.31 26.27
Minimum	8.84	2.17	6.47	6.25	7.26	7.45	5.56	5.28 1.34
Average	25.65	13.92	13.69	13.79	15.40	16.36	18.52	14.78 11.44

5 Conclusion

1. Slug flow, agitation flow and annular flow are the main flow patterns in inclined wellbore with middle and high yield and high gas-liquid ratio. The current flow pattern maps are not suitable for judging flow patterns in this condition, and the new transition boundary of flow patterns is established according to experimental conditions.
2. At the same liquid volume flow rate, liquid holdup decreases with the increase of gas volume flow rate; at the same gas volume flow rate, the liquid holdup rate increases with the increase of liquid volume flow rate. At the same gas volume flow rate, the pressure drop increases with the increases of liquid volume flow rate. At the same liquid volume flow rate, the pressure drop increases with the increase of gas volume flow rate.
3. Evaluate five commonly used pressure drop calculation models and the new model. The prediction errors of the new models for liquid holdup and pressure drop are all about 10%. The prediction of liquid holdup and pressure drop in inclined wellbore is accurate under the conditions of middle and high yield and high gas-liquid ratio.
4. By comparing and verifying the commonly pressure drop calculation models and the new model established in several field measured wells, it is found that the maximum error, minimum error and average error of the new model calculation are small, which proves that the new model is reliable in predicting wellbore pressure and has high accuracy in predicting wellbore pressure.

Acknowledgement: The authors like to express appreciation to the support given by the major national science and technology special project: National Natural Science Foundation of China “Complex System Identification and Optimum Design Based on Hybrid Data and Its Application in Low Permeability Oil Wells” (No. 61572084), National Major Project “Lifting Technology and Matching Technology for Production Wells in Whole Life Cycle” (2016ZX056004-002) and National Major Science and Technology Project (2017ZX05030-005).

Funding Statement: The author(s) received no specific funding for this study.

Conflicts of Interest: The authors declare that they have no conflicts of interest to report regarding the present study.

References

- Barnea, D.** (1986): Transition from annular and from dispersed bubble flow-unified models for whole range of pipe inclinations. *International Journal of Multiphase Flow*, vol. 12, no. 5, pp. 35-36.
- Barnea, D.** (1987): A unified model for predicting flow-pattern transitions for the whole range of pipe inclinations. *International Journal of Multiphase Flow*, vol. 13, no. 1, pp. 1-12. DOI 10.1016/0301-9322(87)90002-4.
- Beggs, D. H.; Brill, J. P.** (1973): A study of two-phase flow in inclined pipes. *Journal of Petroleum Technology*, vol. 25, no. 5, pp. 607-617. DOI 10.2118/4007-PA.
- Bendiksen, K. H.** (1984): An experimental investigation of the motion of long bubbles in inclined tubes. *International Journal of Multiphase Flow*, vol. 10, no. 4, pp. 467-483. DOI 10.1016/0301-9322(84)90057-0.
- Brill, J. P.; Beggs, D. H.** (1986): *Two-phase flow in pipes*. University of Tulsa, USA.
- Chen, J. L.; Chen, T. P.** (2010): *Petroleum gas-liquid two-phase pipe flow*. Petroleum Industry Press, China.
- Gomez, L. E.; Shoham, O.; Schmidt, Z.; Chokshi, R. N.; Northug, T.** (2000): A unified mechanistic model for steady-state two -phase flow: horizontal to vertical upward flow. *SPE Journal*, vol. 5, no. 3, pp. 312-317.
- Han, H. S.; Chen, J. L.** (1986): Flow law of gas-liquid two-phase bubble flow in vertical pipe. *Natural Gas Industry*, vol. 4, no. 6, pp. 58-64.
- Han, H. S.; Chen, J. L.** (1989): Flow law of gas-liquid two-phase slug flow and slug flow in vertical pipe. *Natural Gas Industry*, vol. 1, no. 5, pp. 42-45.
- Han, H. S.; Zhang, H. X.; Xu, X. K.; Shi, Y. X.** (2015): Experimental study on the flow pattern of two-phase flow in inclined pipe. *Contemporary Chemical Industry*, vol. 44, no. 4, pp. 709-710.
- Hasan, A. R.; Kabir, C. S.** (1988): A study of multiphase flow behavior in vertical wells. *SPE Production Engineering*, vol. 3, no. 2, pp. 263-272. DOI 10.2118/15138-PA.

Kabir, C. S.; Hasan, A. R. (1990): Performance of a two-phase gas-liquid flow model in vertical well. *Journal of Petroleum Science and Engineering*, vol. 4, no. 3, pp. 273-289. DOI 10.1016/0920-4105(90)90016-V.

Kaya, A. S.; Sarica, C.; Brill, J. P. (1999): Comprehensive mechanistic modeling of two-phase flow in deviated wells. *SPE Journal*, vol. 4, no. 4, pp. 342-348.

Kaya, A. S.; Sarica, C.; Brill, J. P. (2001): Mechanistic modeling of two-phase flow in deviated wells. *SPE Production & Facilities*, vol. 16, no. 3, pp. 156-165. DOI 10.2118/72998-PA.

Liang, Y. (2019). *A study of liquid-carrying mechanism and pressure drop characteristics of gas-liquid two-phase flow in inclined wells (Ph.D. Thesis)*. Xian Petroleum University, Xi'an.

Mukherjee, H.; Brill, J. P. (1985): Pressure drop correlations for inclined two-phase flow. *Journal of Energy Resources Technology*, vol. 4, no. 4, pp. 549-554. DOI 10.1115/1.3231233.

Tengesdal, J. O.; Kaya, A. S.; Sarica, C. (1999): Flow-pattern transition and hydrodynamic modeling of churn flow. *Society of Petroleum Engineers*, vol. 36, no. 6, pp. 333-342.

Zhang, X. (2015). *Numerical Simulation and Experiment Research on Flow Pattern of Gas-liquid Two-phase Flow in Upward Inclined Pipe (Ph.D. Thesis)*. Northeast Petroleum University, Daqing.

Zhang, H. Q.; Wang, Q.; Sarica, C.; Brill, J. P. (2003): A unified mechanistic model for slug liquid holdup and transition between slug and dispersed bubble flows. *International Journal of Multiphase Flow*, vol. 29, no. 1, pp. 97-107. DOI 10.1016/S0301-9322(02)00111-8.

Zhou, S. Z.; Zhu, L.; Zhang, Y. B.; Zheng, W. (2016): Experimental study of two-phase flow in inclined pipe under high gas-liquid flow. *Contemporary Chemical Industry*, vol. 45, no. 3, pp. 504-506.